


# What caused the spring intensification and winter demise of the 2011 drought over Texas?

D. Nelun Fernando<sup>1,2,3</sup>  · Kingtse C. Mo<sup>4</sup> · Rong Fu<sup>2</sup> · Bing Pu<sup>2,8</sup> · Adam Bowerman<sup>2</sup> · Bridget R. Scanlon<sup>5</sup> · Ruben S. Solis<sup>3</sup> · Lei Yin<sup>2</sup> · Robert E. Mace<sup>3</sup> · John R. Mioduszewski<sup>6,9</sup> · Tong Ren<sup>2,7</sup> · Kai Zhang<sup>2</sup>

Received: 10 April 2015 / Accepted: 27 January 2016  
© Springer-Verlag Berlin Heidelberg 2016

**Abstract** The 2011 Texas drought, the worst 1-year drought on record, was characterized by spring intensification of rainfall deficit and surface dryness. Such spring intensification was led by an unusually strong increase of convective inhibition (CIN), which suppressed convection at the time critical for the onset of the April–June rainfall season. The CIN increase appeared to be caused by strong sub-seasonal anomalously westerly winds at 850 hPa (U850) in April, in

addition to surface dryness due to cumulative rainfall deficit since fall of 2010. The anomalous U850 advected warm dry air from the Mexican Plateau to Texas, enhancing cap inversion, and exacerbating static stability initially elevated by an anomalously high surface Bowen ratio due to rainfall deficits from winter through spring over Texas. Strengthened westerly U850 in April, in addition to the persistent rainfall deficits from winter through spring, are common characteristics in other strong drought events experienced over Texas. Atmospheric Model Intercomparison Project-type simulations with prescribed La Niña SSTAs in the tropical Pacific do not show a strengthening of westerly U850 in April, suggesting that internal atmospheric variability at intraseasonal scale, instead of La Niña, may initiate the spring drought intensification over Texas. Soil moisture deficits in late spring are significantly correlated with positive 500 hPa geopotential height anomalies over the south central U.S. 2–3 weeks later, suggesting that intensified surface dryness in late-spring could reinforce the drought-inducing anomalous mid-tropospheric high. The drought diminished in the winter of 2011/2012 despite a second La Niña event. Our analysis suggests an important role for strong westerly wind anomalies, the resultant increase of CIN in spring, and subsequent positive feedback between dry surface anomalies and the anomalous large-scale circulation pattern in drought intensification. Clarification of the mechanisms behind the strong increase of CIN and land–atmosphere feedbacks may provide a key for improving our understanding of drought predictability in spring and summer, and a scientific basis for the early warning of strong summer drought. The demise of the 2011 drought appears to have resulted from internal atmospheric circulation variability, thus intrinsically unpredictable.

**Electronic supplementary material** The online version of this article (doi:10.1007/s00382-016-3014-x) contains supplementary material, which is available to authorized users.

✉ D. Nelun Fernando  
Nelun.Fernando@twdb.texas.gov

<sup>1</sup> University Corporation for Atmospheric Research, Boulder, CO 80307, USA

<sup>2</sup> Department of Geological Sciences, Jackson School of Geosciences, University of Texas at Austin, Austin, TX 78712, USA

<sup>3</sup> Present Address: Water Science and Conservation, Texas Water Development Board, Austin, TX 78701, USA

<sup>4</sup> Climate Prediction Center, NOAA/NWS/NCEP, College Park, MD 20740, USA

<sup>5</sup> Bureau of Economic Geology, Jackson School of Geosciences, University of Texas at Austin, J.J. Pickle Research Campus, Austin, TX 78758, USA

<sup>6</sup> Department of Geography, Rutgers University, Piscataway, NJ 08854, USA

<sup>7</sup> Present Address: Department of Atmospheric and Oceanic Sciences, Texas A&M, College Station, TX, USA

<sup>8</sup> Present Address: Department of Atmospheric and Oceanic Sciences, Princeton University, Princeton, USA

<sup>9</sup> Present Address: Center for Climatic Research, University of Wisconsin-Madison, Madison, USA

**Keywords** Drought · Spring intensification · Convective inhibition · Soil moisture · La Niña · Texas

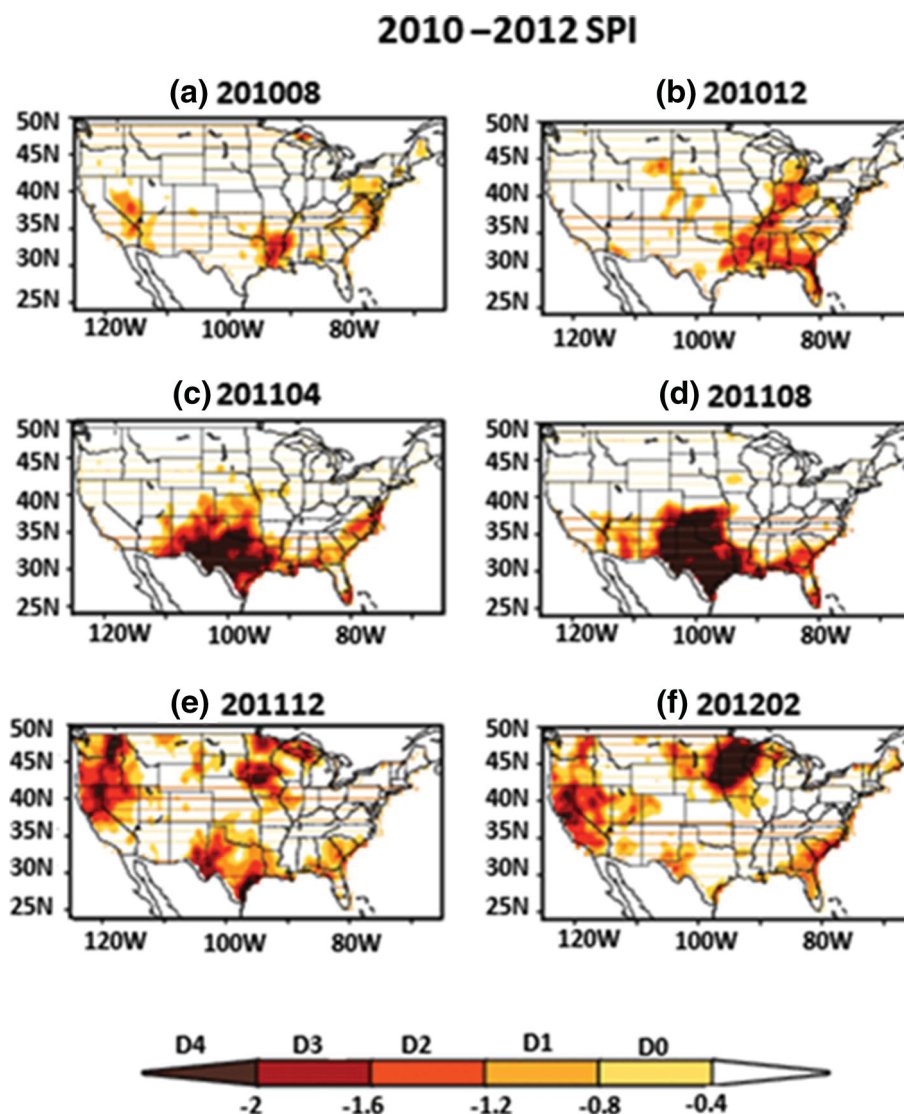
## 1 Introduction

In 2011, Texas suffered its worst drought in recent decades. Drought conditions are illustrated by the 6-month standardized precipitation index (SPI6, Fig. 1). Drought started over the eastern Texas in the winter of 2010/2011 (Fig. 1b). In spring 2011, drought suddenly intensified over most areas in Texas (Fig. 1c). Drought lasted through summer and ended in the 2011/2012 winter. The economic impact of this drought on Texas is estimated at 7.6 billion dollars (Fannin 2012) primarily from crop and livestock losses. In addition to drought, there was record heat in the summer with a mean temperature (JJA) of 30.4 °C, which was 2.9 °C higher than climatology (Hoerling et al. 2013). The rapid spring intensification of the 2011 drought caused statewide reservoir storage to drop to 58 % in November 2011, which was the lowest since 1978 (Texas Water

Development Board 2010, 2011a, b). The meteorological drought ended unexpectedly with a wet winter (2011/2012) (Fig. 1e, f).

Droughts in Texas tend to occur during cold El Niño Southern Oscillation (ENSO)—(La Niña)—events (Ropelewski and Halpert 1989), although La Niña does not always lead to summer droughts in this region. Hoerling et al. (2013) have attributed precipitation deficits in the 2011 drought to sea surface temperature anomalies (SSTAs) associated with the La Niña, which set up antecedent and concurrent conditions for the record breaking heat wave in summer 2011. For 2011, negative SSTAs in the tropical Pacific indicated La Niña conditions in winter (Fig. 2). By summer, the La Niña induced SSTAs had mostly diminished (less than  $-0.5$  °C), but rainfall deficit persisted and drought reached its peak intensity. La Niña reappeared in September–November (SON) of 2011 and lasted through the 2011/2012

**Fig. 1** The evolution of drought, depicted using the 6-month standardized precipitation index (SPI6), for **a** August 2010, **b** December 2010, **c** April 2011, **d** August 2011, **e** December 2011, and **f** February 2012. The Drought Monitor D0–D4 categories associated with SPI6 values are provided in the scale bar



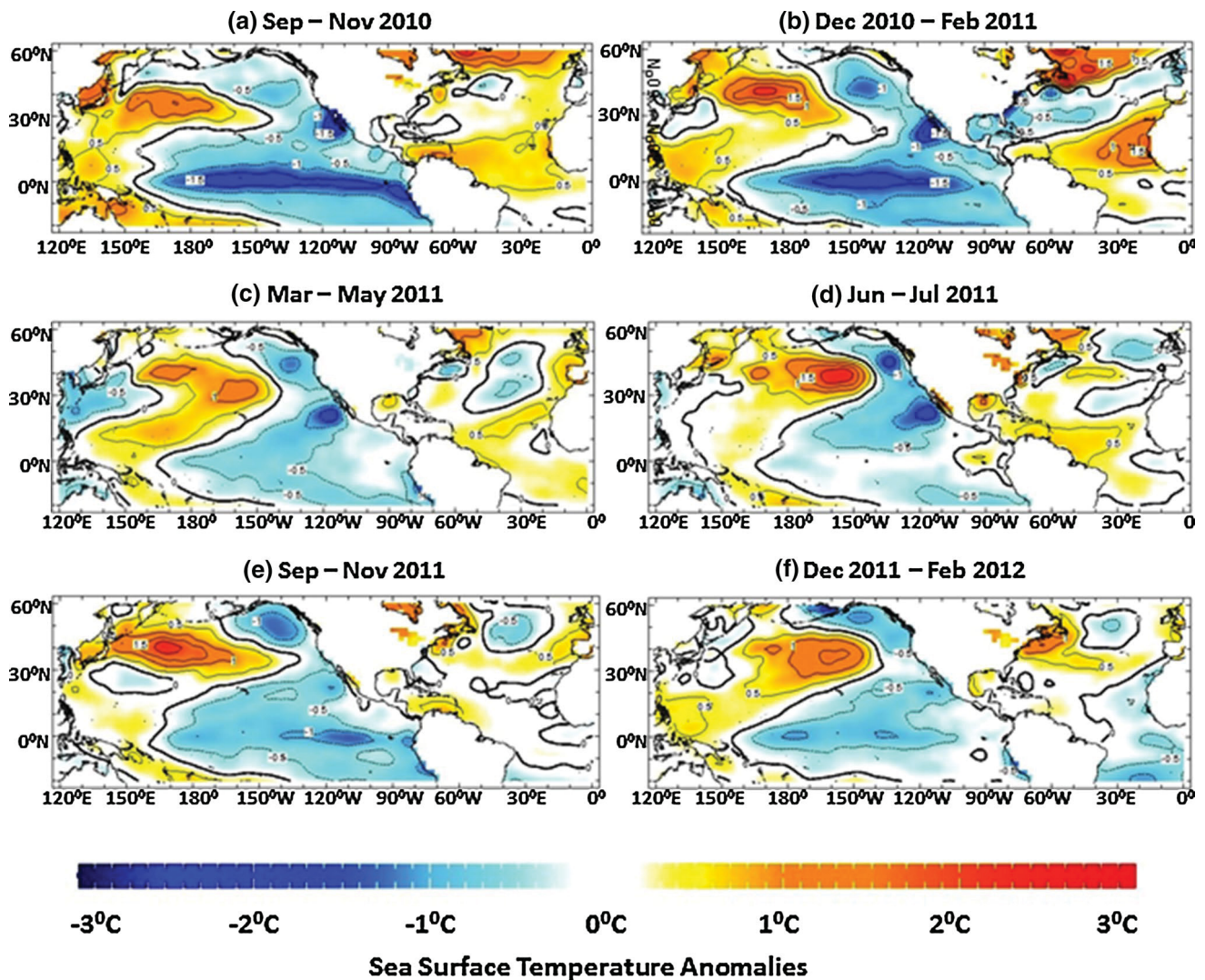


**Fig. 2** SSTAs during **a** the onset of the 2010 La Niña event in the fall (SON) of 2010, **b** the La Niña peak in winter (DJF) of 2010/2011, **c** the weakening of the La Niña event in spring (MAM) 2011, **d** ENSO neutral conditions in summer (JJA) of 2011, **e** onset of the 2011 La

Niña event in SON 2011, and **f** the La Niña peak in DJF 2011/2012. *Solid contours* denote warmer SSTAs and *dashed contours* denote cooler SSTAs. Contour interval is 0.1 °C

winter when drought conditions improved. The correspondence between ENSO and drought intensification and demise remains unclear for this event.

In addition to La Niña, the SSTAs in the North Pacific (Ting and Wang 1997; Barlow et al. 2001) and the Atlantic SSTAs can also (Enfield and Mayer 1997; McCabe et al. 2008; Hu and Feng 2012) influence rainfall over the south central United States. Positive SSTAs in the tropical Atlantic also enhance the impact of La Niña events on precipitation over the southern United States (Mo et al. 2009; Schubert et al. 2009). Seager et al. (2014) indicated that SSTAs in the North Atlantic may have played a role in the 2011 drought. Based on these previous studies, SSTAs in the Pacific and the Atlantic appear to have played a role in initiating and sustaining the drought from the winter

of 2010/2011 into the spring of 2011, but their role in the spring intensification is less evident.

Internal atmospheric variability or strong local land–atmosphere coupling could also have played a role in driving such drought intensification (Seager et al. 2014). The southern Great Plains region is one of the hot spots where land–atmosphere interaction is strong (Koster et al. 2004). For example, Hong and Kalnay (2002) found that land–atmosphere interaction and feedback contributed to drought over Texas in 1998.

Local thermodynamic conditions may also play a role in maintaining and enhancing drought. Myoung and Nielsen-Gammon (2010) identified convective inhibition (CIN) as the primary condition that controls summer drought over Texas. CIN has a major influence on precipitation deficits



on monthly time scales and is caused by high surface temperature, surface dryness (i.e. soil moisture deficits) and warming in the mid-troposphere (Myoung and Nielsen-Gammon 2010). CIN can be influenced by an increase of surface dew point depression and an increase of temperature above the atmospheric boundary layer (ABL) (Myoung and Nielsen-Gammon 2010). These conditions can be influenced either by diabatic heating/cooling, vertical heat transport, or by horizontal advection. The role of CIN in the development and intensification of drought in the spring over Texas has not been investigated.

Understanding factors that led to the spring intensification and unexpected demise of the 2011 drought is critical in determining potential drought predictability and the feasibility of drought early warning. While many previous studies have examined the causes of the 2011 drought, the causes for its spring intensification are still unclear. In this paper, we will explore the remote and local processes associated with the strengthening of the drought in the spring and its quick demise in the winter of 2011/2012. We first examine the anomalous circulation patterns in spring and summer and their relationship with SSTAs, particularly in the tropical Pacific.

Next, we study the anomalous local thermodynamic structure and examine factors driving the evolution of CIN during the drought. We finally examine the relationship between local surface dryness and large-scale circulation anomalies to infer the causes of drought intensification and persistence.

## 2 Datasets and methods

We examined the evolution of the drought over Texas from the late fall of 2010 through summer 2011 using the 6-monthly Standardized Precipitation Index (SPI6) (McKee et al. 1993; McKee et al. 1995) using the Climate Prediction Center (CPC) unified precipitation data set (Xie et al. 2010). The horizontal resolution of the dataset is 0.5 degrees.

The associated SSTAs in the Pacific and Atlantic Ocean basins were obtained using the Extended Reconstructed Sea Surface Temperature version 3b (Smith et al. 2008), available at  $2^\circ \times 2^\circ$  resolution. We used the 3-month Oceanic Niño Index from the Climate Prediction Center ([http://www.cpc.ncep.noaa.gov/products/analysis\\_monitoring/ensostuff/ensoyears.shtml](http://www.cpc.ncep.noaa.gov/products/analysis_monitoring/ensostuff/ensoyears.shtml)) to obtain the 3-monthly Niño3.4 index for La Niña years.

We determined convection anomalies using the outgoing longwave radiation (OLR) from the CPC global monthly outgoing longwave radiation dataset (Liebmann and Smith 1996) available at  $2.5^\circ \times 2.5^\circ$  resolution. Most of the large scale circulation anomalies (e.g. relative vorticity) and thermodynamic properties such as CIN were obtained or derived from

the National Centers for Environmental Prediction (NCEP) reanalysis (Kalnay et al. 1996), available at  $2.5^\circ \times 2.5^\circ$  resolution. The European Center for Medium-Range Weather Forecasting ERA-Interim Reanalysis (Dee et al. 2011) at  $0.7^\circ \times 0.7^\circ$  horizontal and 6-hourly temporal resolutions was used to compute horizontal and vertical heat advection.

We used surface temperature data from the CPC monthly global surface temperature dataset (Fan and van den Dool 2008) available at  $0.5^\circ \times 0.5^\circ$  resolution.

Past drought years were identified using the 12-monthly Standardized Precipitation Index for August (August SPI12) averaged over Texas from the National Climatic Data Center (NCDC) climate indices dataset (<http://www7.ncdc.noaa.gov/CDO/CDODivisionalSelect.jsp#>). In the study of historical drought, we focused on drought at the longer time scale (i.e. 12-month time scale), hence the reason for using the 12-month SPI. While tracking the evolution of drought (discussed above) over Texas during the 2011 event we used the 6-month SPI because our purpose was to explain drought establishment, persistence, and demise over Texas within a finite time period. Seasonal rainfall anomalies in all strong drought events over Texas, defined as the state-wide 12-month Standardized Precipitation Index being less than  $-1.2$ , from 1895 to the present were obtained using the monthly rainfall product from PRISM (<http://www.prism.oregonstate.edu/>) available at 4 km resolution. The domain used for the PRISM dataset is  $106.8^\circ\text{W}$  to  $93.5^\circ\text{W}$  and  $25.5^\circ\text{N}$  to  $36.8^\circ\text{N}$ .

To investigate the relationship between La Niña and the strength of the westerly winds over Texas in April, we conducted SST experiments using the National Center for Atmospheric Research (NCAR) Community Atmospheric Model version 5.3 (CAM5.3, Neale et al. 2012) with prescribed SSTAs. The control experiment was run with climatological SSTs from the HadISST (Rayner et al. 2003) averaged over 1950–2012. The second experiment was run with La Niña-type SSTAs (La Niña test run). The comparison between the two runs would reveal the influence of La Niña on the anomalous large scale circulation in April. The SSTAs for the second experiment were obtained for each month by averaging the tropical Pacific SSTA ( $20.5^\circ\text{S}$ – $20.5^\circ\text{N}$ ) over the strongest 25 % (i.e., 36 years; selected based on monthly SSTAs averaged over the Niño 3.4 area) La Niña years during 1870–2013. The 12 monthly mean La Niña-type SSTAs are then added to the climatological monthly SST to drive the model. We have 7 years (7) of the control run and twenty-one (21) years of the La Niña test run. The first year from the control run and first 6 years from the La Niña run are discarded for spin-up, and results are presented by averaging over the rest of the years.

Land surface variables at monthly time steps such as evaporation anomalies, total column (200 cm) soil moisture percentiles and sensible heat anomalies were derived from

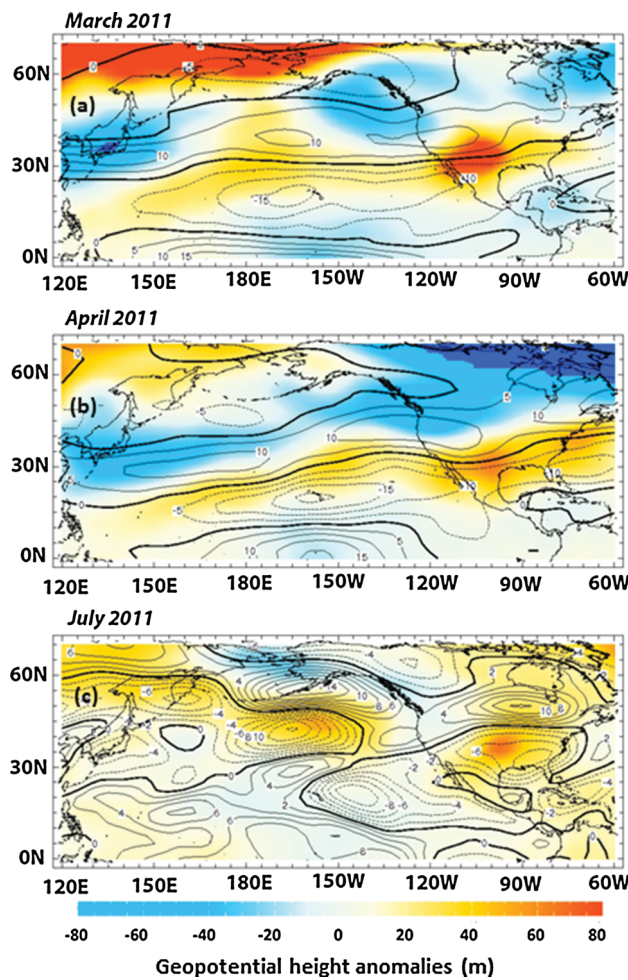


**Fig. 3** a The zonal asymmetric 200 hPa geopotential height anomalies superimposed by 1000–500 hPa thickness anomalies in March 2011. Contour interval for 200 hPa height anomalies is 5 m and shading intervals for the 1000–500 hPa thickness is 20 m. **b** As in **a** but for April 2011. **c** As in **b** but for July 2011

ensemble means of the VIC, Noah and Mosaic model output in the NCEP North American Land Data Assimilation System (NLDAS Xia et al. 2012) for the period 1979–2012. Total column soil moisture at the pentad timescale was derived using hourly soil moisture from the NLDAS Noah model.

To determine the source of temperature increases in the atmospheric boundary layer, we analyzed each term of the thermodynamic energy equation (Eq. 1) to determine their relative importance.

$$\frac{\partial \bar{T}}{\partial t} = \frac{\bar{Q}}{C_p} - \left(\frac{p}{p_0}\right)^\kappa \bar{\omega} \frac{\partial \bar{\theta}}{\partial p} - \bar{v} \cdot \nabla_p \bar{T} - \left(\frac{p}{p_0}\right)^\kappa \frac{\partial}{\partial p} (\bar{\omega}'\theta') - \nabla_p \cdot (\bar{v}'T')$$
(1)

where the “ $\bar{\cdot}$ ” denotes monthly mean and “ $\cdot$ ” denotes 6 h perturbation. These terms from left to right represent

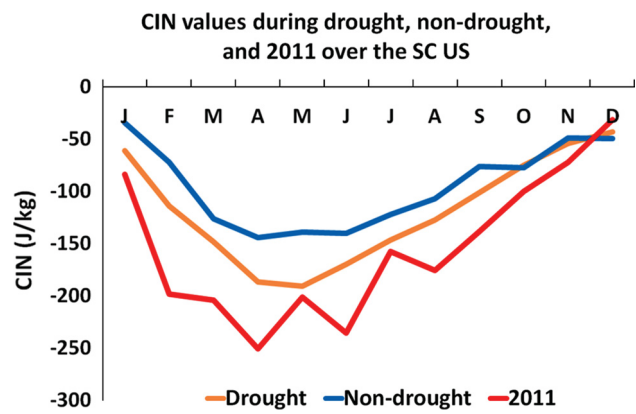


**Fig. 4** Comparative plot of monthly CIN values over the domain 24°N–40°N and 110°W–92°W during 2011 (red), composite CIN in past severe-to-extreme drought events (brown) over the same domain since 1950, and CIN in non-drought years (blue). The CIN values in the spring of 2011, particularly in April 2011, were larger than the composite mean CIN for past droughts. CIN values are about 50 J/kg less in April–May of non-drought years

the time mean rate of temperature change, diabatic heating, vertical advection of potential temperature, horizontal advection of temperature, and the perturbation terms for vertical and horizontal advection, respectively. The perturbation zonal advection term was neglected because it is comparatively small at the monthly time scale. We used 6-hourly horizontal temperature and zonal and meridional wind data obtained from ERA-Interim to compute each term. The 6-hourly values are then aggregated to monthly values.

We also studied the surface temperature anomaly and the 850 hPa relative vorticity anomaly for April 2011 to distinguish between a local forced diabatic response and a non-local dynamical structure to the observed relative vorticity anomaly at 850 hPa over Texas in April 2011.

To address how local land surface characteristics in the spring might influence mid-tropospheric stability in the summer, we use lead-lag correlation analysis using pentad total column soil moisture anomalies and geopotential height from May through July (MJJ). Soil moisture and geopotential height anomalies are obtained by subtracting the seasonal means for each pentad and detrending both time series. In addition, the annual and semi-annual harmonics are removed from the 500 hPa geopotential height anomaly field to remove the periodic seasonal signal from the data. We account for autocorrelation in both time series by estimating the effective number of independent samples (Livezey and Chen 1983) prior to estimating the 95 % confidence bounds. We also test whether the lead-lag correlation is significantly different to the autocorrelation in the 500 hPa geopotential height anomaly field by using the z test for differences of mean under serial dependence (Wilks

2006). We use a base period of 1979–2012 to compute anomalies for all the variables.

### 3 Results

#### 3.1 Drought intensification in spring and summer

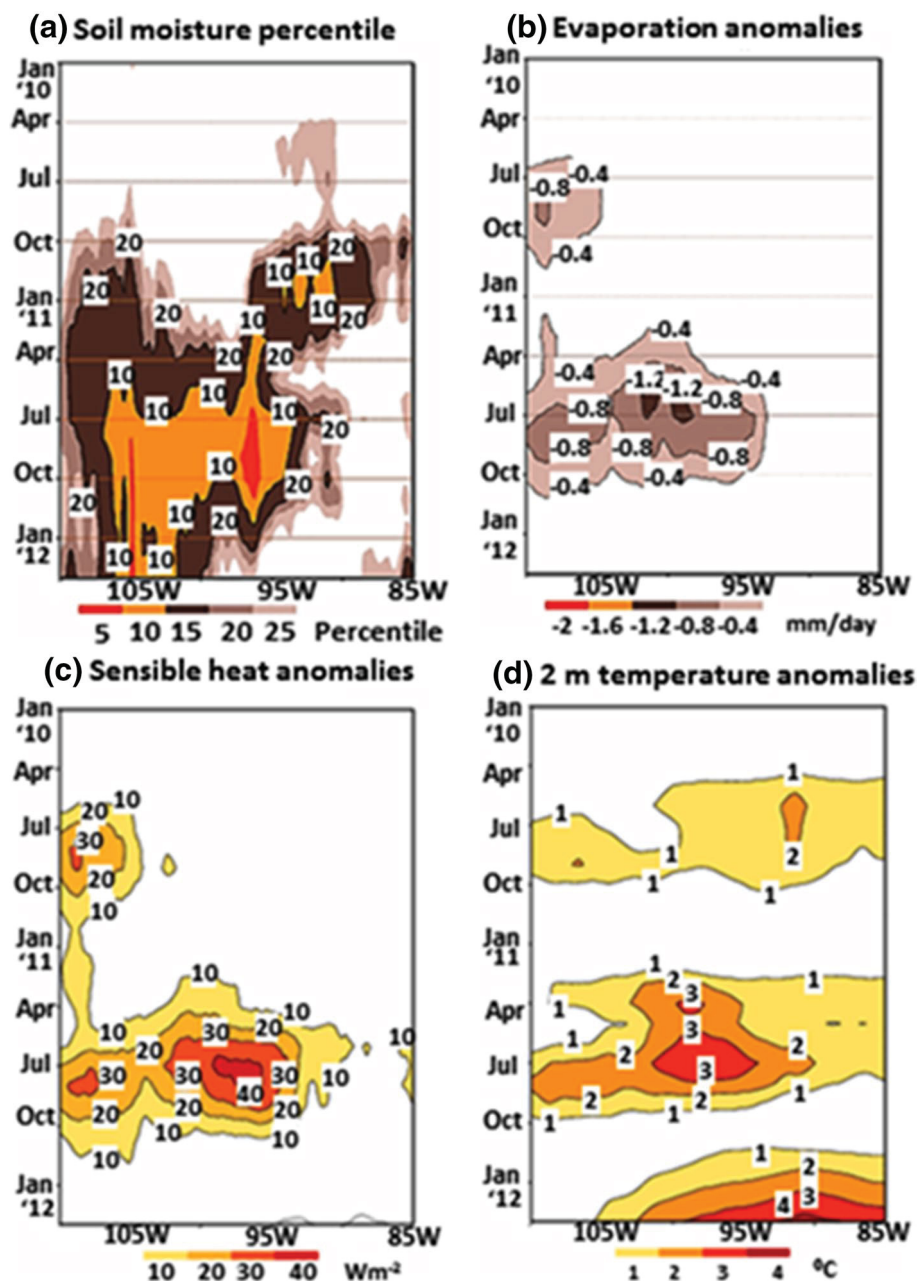
##### 3.1.1 Anomalous circulation in spring and summer and relationship to SSTAs

The La Niña induced negative SSTAs over the central and eastern equatorial Pacific were accompanied by negative

SSTAs off the west coast of North America, from September 2010 to February 2011 (Fig. 2a, b). The La Niña weakened substantially in the spring of 2011 (Fig. 2c). SSTAs in the tropical Pacific were at ENSO-neutral conditions in the summer of 2011 (Fig. 2d). However, negative SSTAs off the west coast of North America persisted through the spring and summer of 2011 (Fig. 2c, d). La Niña SSTAs reappeared from September 2011 to February 2012 (Fig. 2e, f).

In a typical response to convective anomalies associated with a La Niña event, the sub-tropical jet stream is displaced poleward. This deflects the winter storm tracks north of their climatological location and causes a reduction of

**Fig. 5** The evolution of land surface conditions, averaged over 20°N–40°N, as the drought progressed depicted with a time-longitude plot for soil moisture percentiles, with contour interval of 5 percentiles, **b** same as **a** but for evaporation anomalies with contour interval of 0.1 mm/day, **c** As in **b** but for sensible heat anomalies, with contour interval of 10 Wm<sup>-2</sup>, and **d** As in **c** but for 2-m (T2m) temperature anomalies, with contour interval of 2 °C





precipitation over the southern Great Plains (Eichler and Higgins 2006; Kousky and Ropelewski 1989). Such an anomalous circulation pattern occurred in March and April of 2011 (Fig. 3a, b), although the mean SSTA for the spring along the equator was only  $-0.4\text{ }^{\circ}\text{C}$  (Fig. 2c). The outgoing longwave radiation (OLR) anomalies for March-to-May (MAM) (Supplementary 1) indicate enhanced convection in the western Pacific, as expected during a La Niña event. The sub-tropical jet stream was displaced poleward in March and April 2011, as depicted by positive 200 hPa zonal wind anomalies over the northwestern US and negative 200 hPa zonal wind anomalies over the southern regions of North America (Fig. 3a, b). The poleward shift of the jet stream during March–April (Fig. 3a, b) would reduce synoptic disturbances and contribute to dryness over the southern plains in the early spring. In May 2011, the jet stream is located over the southern U.S. (not shown).

The increase of zonal asymmetric 1000–500 hPa thicknesses (Fig. 3, orange shading) over the southwestern and south central US suggest anomalous warmth from the surface to the mid-troposphere in March and April 2011 (Fig. 3a, b). The combination of such increased lower troposphere thickness over southern US and decreased thickness over North Pacific and northwestern North America led to an increased meridional geopotential gradient, and could have strengthened the zonal wind in the lower

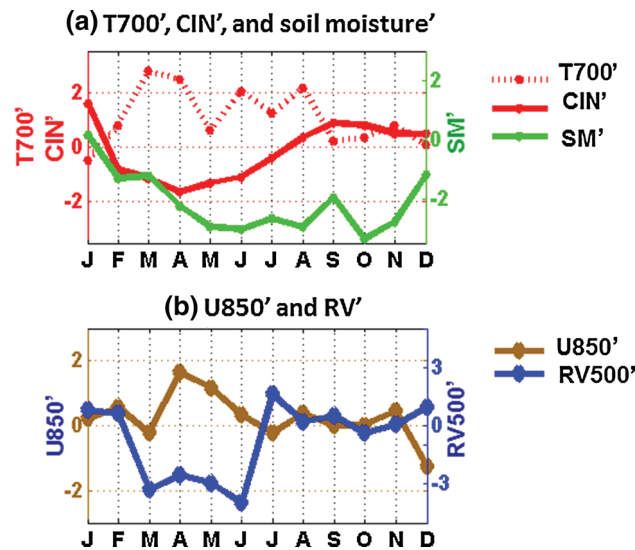


**Fig. 6** a Anomalous temperature at 700 hPa (dash-red), soil moisture percentile (green) and CIN anomalies (solid red) over the domain  $24^{\circ}\text{N}$ – $40^{\circ}\text{N}$  and  $110^{\circ}\text{W}$ – $92^{\circ}\text{W}$  from January to December 2011. The steady increase of soil moisture deficit from March through June 2011 probably contributed to the increase of CIN magnitude (red) in spring 2011. However, variation of CIN appear to follow the increase of temperature at 700 hPa more closely from March to April; and b the strong westerly wind anomalies at 850 hPa (brown) and negative relative vorticity (RV) anomalies (blue) at 500 hPa during April and May, and March to June, respectively, in 2011

troposphere in March–April. By July 2011, above normal thickness anomalies have a local maximum over central and northern Texas and the Oklahoma region (Fig. 3c), when the jet stream is again displaced poleward

3.1.2 Anomalous local thermodynamic structure in the late-spring

The importance of CIN as a main cause of summer droughts over Texas has been shown by Myoung and Nielsen-Gammon (2010). We find that unusually strong CIN occurred over Texas during from February to May 2011, with a maximum in April 2011 (Fig. 4, red). The monthly CIN value of 2011 exceeded the mean CIN anomaly of other

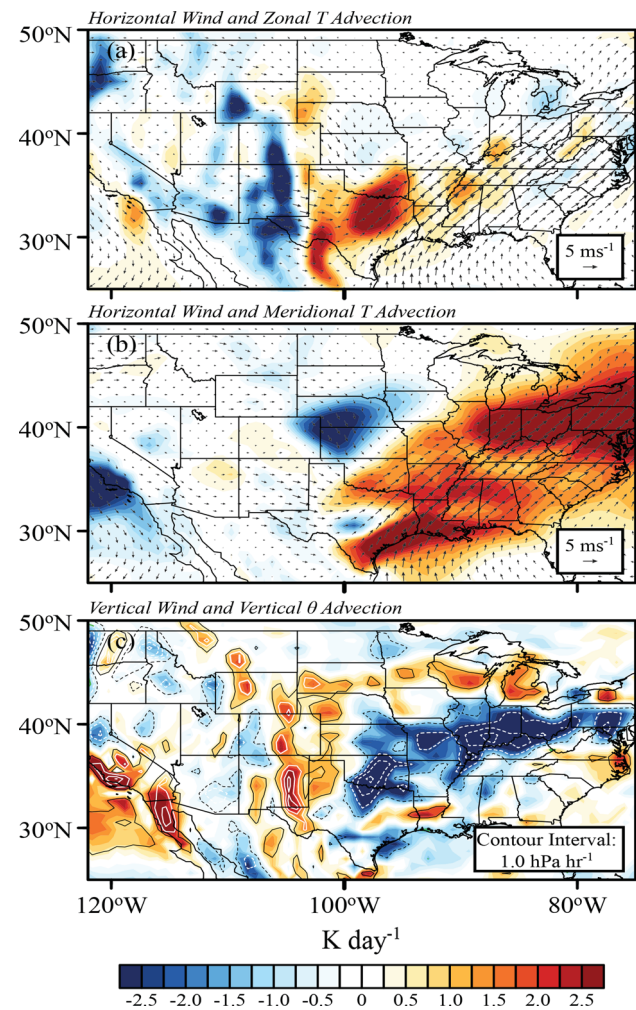


**Fig. 7** a Anomalous zonal heat advection at 850 hPa in April 2011 shows an eastward advection of warm air (red shading) over Texas. b Anomalous meridional advection at 850 hPa in April 2011 shows the northward advection of warm air from the Gulf of Mexico into Louisiana. The vector wind anomaly for April 2011 is overlain on the thermal advection map to provide directionality to the thermal advection. c Anomalous vertical thermal advection in April 2011 shows vertical cooling over northern Texas and Oklahoma

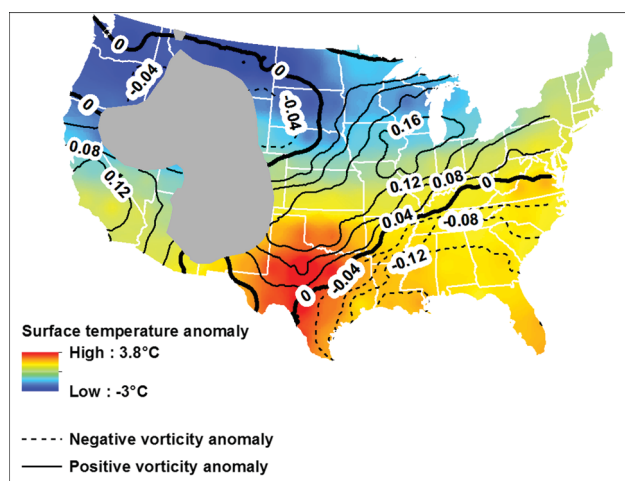


**Fig. 8 a** Monthly mean relative vorticity anomaly at 850 hPa (contours) and surface temperature anomalies (shading) for April 2011 shows positive vorticity (solid contours) over north Texas and negative vorticity (dashed contours) over south eastern Texas. Contour interval is  $0.4 \times 10^{-5} \text{ s}^{-1}$ . Grey shading masks areas over 1.5 km in elevation. Surface temperature anomalies show an area of anomalous warmth (red shading) extending from southwestern to north central Texas

severe-to-extreme drought events experienced over Texas post-1950 (Fig. 5, brown). The strong CIN in spring of 2011 and other drought years contrasts to the lower value of CIN during non-drought years (Fig. 4, blue), and suggests the importance of CIN in spring drought intensification. Figure 4 further suggests that a strong increase in CIN in spring is an important precursor for summer drought.

**Table 1** Strong drought years categorized by seasonal rainfall anomaly state and La Niña (LN) state (depicted for years post 1950)

Seasonal state transition	Years
DJF <sub>(dry)</sub>  MAM <sub>(dry)</sub>  JJA <sub>(dry)</sub> :	1909, 1910, 1917, 1918, 1925, 1951 (LN), 1954(LN), 1955(LN), 1956(LN), 1967, 2006(LN),2011(LN)
DJF <sub>(wet)</sub>  MAM <sub>(dry)</sub>  JJA <sub>(dry)</sub> :	1896
DJF <sub>(dry)</sub>  MAM <sub>(wet)</sub>  JJA <sub>(dry)</sub> :	2000(LN)

A year is classified as a La Niña year based on the onset or demise season of a La Niña event (e.g. if an event ended in DJF, the following April of that year was selected as a target for inclusion as a La Niña April; if an event onset was in AMJ, the April of that year was also selected as a target for inclusion as a La Niña April). Historical El Niño and La Niña events were identified from based on CPC's classification ([http://www.cpc.ncep.noaa.gov/products/analysis\\_monitoring/ensostuff/ensoyears.shtml](http://www.cpc.ncep.noaa.gov/products/analysis_monitoring/ensostuff/ensoyears.shtml))

Percentage of dry springs preceding summer drought: **12 out of 13 = 92 %** (only in the drought year 2000 was the winter rainfall deficit terminated by a wet spring)

Year(s) when La Niña induced winter drought that ended in spring: 1 (i.e. 2000)

What factors led to the increase of CIN in spring 2011? We analyze whether the rainfall deficit from winter through spring led to an increase in sensible heating over Texas in the spring and summer of 2011. With the lack of rain in the 2010/2011 winter, soil moisture anomalies over east Texas and the south eastern U.S. ( $85^{\circ}\text{W}$ – $95^{\circ}\text{W}$ ) and over New Mexico ( $105^{\circ}\text{W}$ – $110^{\circ}\text{W}$ ) to the west of Texas reached their lowest 15th percentile in October 2010, but they did not appear to influence evapotranspiration (ET) significantly. Over Texas ( $95^{\circ}\text{W}$ – $105^{\circ}\text{W}$ ), soil moisture decreased to the lowest 25th percentile (Fig. 5a, orange shading) in April 2011 and reached the lowest 10th percentile in June (Fig. 5a, red shading). The soil moisture decrease over Texas appears to have led to a strong decrease of ET (Fig. 5b). The sensible heat flux increased (Fig. 5c) to balance the decrease in ET, resulting in positive surface temperature anomalies in Texas and New Mexico centered over central Texas (Fig. 5d, red shading). This is consistent with the inverse relationship between precipitation and surface temperature reported in previous studies (e.g. Namias 1960; Madden and Williams 1978; Trenberth and Shea 2005).

Are there other causes for the strong increase of CIN? The increase of CIN follows the warming at 700 hPa more closely than soil moisture anomalies (Fig. 6a). The former could enhance the cap inversion and CIN (Myoung and Nielsen-Gammon 2010). The warm anomalies at 700 hPa occurred concurrently with negative relative vorticity (RV) anomalies at 500 hPa during March–June, and anomalously strong westerly winds at 850 hPa during April–June (Fig. 6b). The analysis of temperature advection and wind shows that the zonal warm temperature advection due to enhanced westerlies at 850 hPa is much stronger than meridional and vertical temperature advectons over central and northeastern Texas in April 2011 (Fig. 7a). The meridional warm advection dominates the temperature advection over the Texas southern coast and other states along the central Gulf Coast (Fig. 7b), and the vertical advection of cooler temperature over limited area in the northeastern Texas nearly compensated the warm zonal temperature advection (Fig. 7c).

Analysis of vorticity anomalies at 850 hPa and surface temperature anomalies for April show a region of maximum positive vorticity (Fig. 8, solid contours) over the Texas Panhandle, which extends over Oklahoma and north-eastward over the Midwestern states; maximum negative vorticity over southeastern Texas and Louisiana (Fig. 8a, dashed contours); and a maximum surface temperature anomaly extending from southwestern Texas through northeastern Texas (Fig. 8, red shading). The analysis of 850 hPa geopotential height anomalies in April 2011 indicate the presence of a lee trough structure (Supplementary Figure 2) lying over the region of maximum positive vorticity noted in Fig. 8. The location of the maximum surface



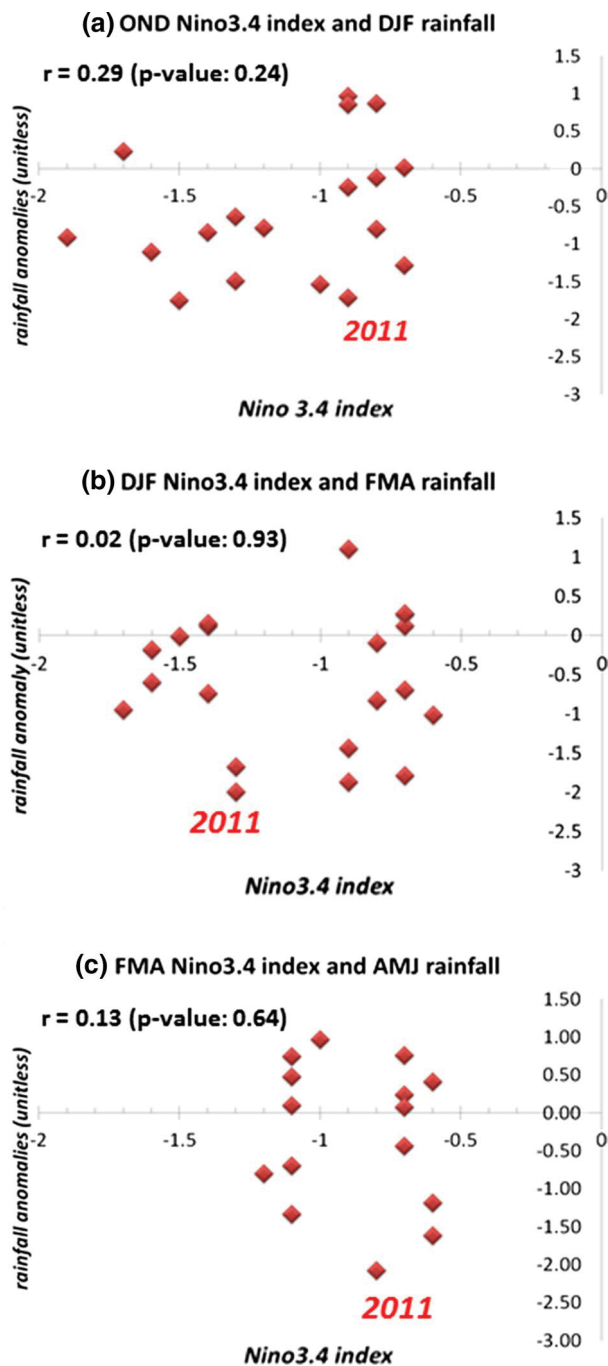


**Fig. 9** Scatter plots depicting strength of 2-month-lead Nino3.4 index in La Niña years and seasonal rainfall departure over Texas for **a** Oct–Nov (OND) Nino3.4 index and Dec–Feb (DJF) rainfall, **b** Dec–Feb (DJF) Nino3.4 index and Feb–Apr (FMA) rainfall, and **c** Feb–Apr (FMA) Nino3.4 index and Apr–Jun (AMJ) rainfall

temperature anomaly and the maximum positive vorticity anomaly at 850 hPa are not co-located, indicating that the non-local dynamical structure has more influence than local diabatic forcing on the observed low-level potential vorticity anomaly in April 2011 over Texas. Past studies note

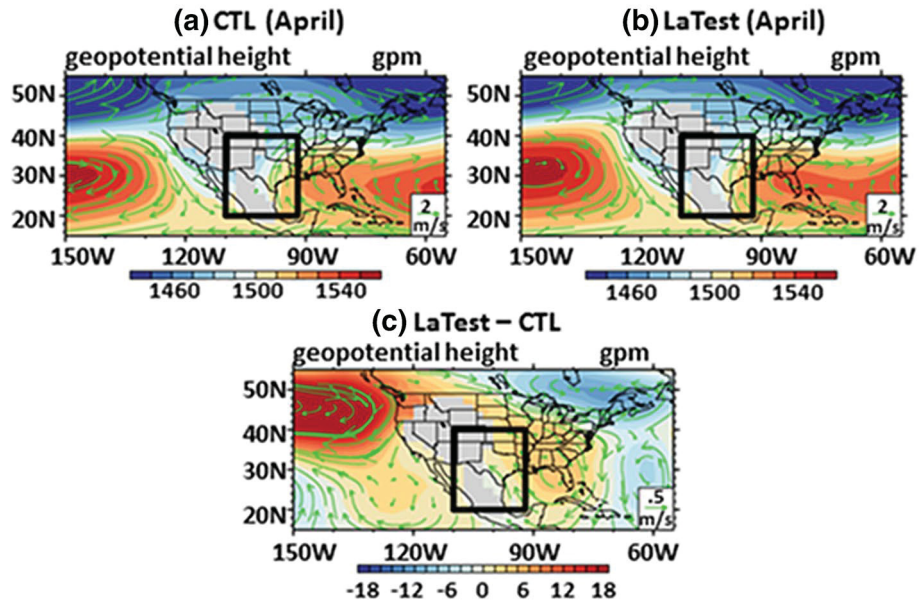
the formation of a cap inversion over Texas in the warm season when winds are blowing at right angles to the Rockies and the Mexican Plateau (Benjamin and Carlson 1986; Weisman 1990 and references there-in). The observed increase in temperature at 850 hPa, and increase in CIN, can be attributed to the adiabatic warming and stretching associated with downslope winds. The heating at 850 hPa was mostly sensible heating. Such low-level warming and the cap inversion suppressed convection and clouds in the late-spring of 2011.

Ninety-two percent of severe-to-exceptional summer droughts experienced from 1985 to 2014, as indicated by the 12-monthly Standardized Precipitation Index for August (August SPI12) being less than  $-1.2$ , were preceded by dry springs (Table 1). Six out of these seven strong summer droughts falling within the post-1950 period (i.e. 1951, 1954, 1956, 1967, 2006, and 2011) were characterized by winter rainfall deficits attributable to La Niña events. In only one drought event (2000) did La Niña-induced winter rainfall deficits end in the spring. Anomalously strong westerlies at 850 hPa in April are characteristic of all 7 severe-to-extreme drought events, from 1951 to the present (i.e. 1951, 1954, 1955, 1956, 1967, 2006 and 2011), with persistent negative rainfall anomalies from winter through summer (Table 1). The observed anomaly in April 2011 was nearly twice its climatological strength (Fig. 6b).

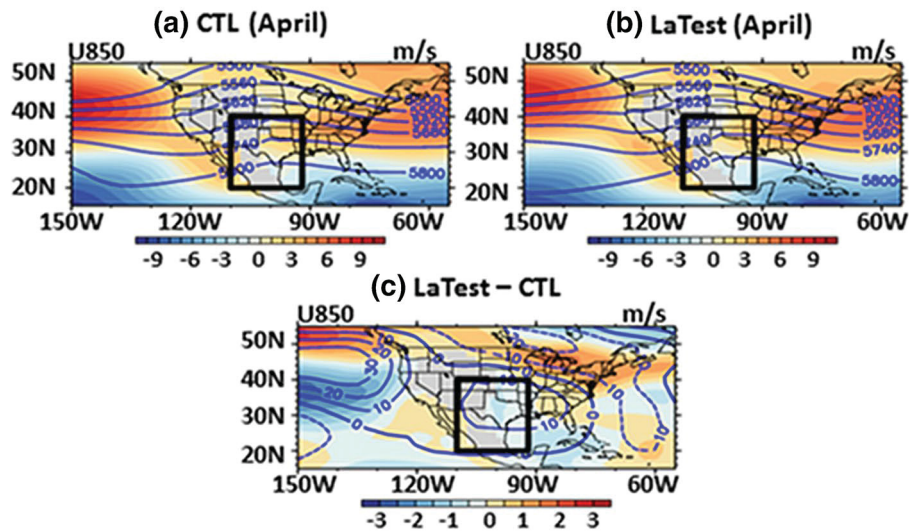
Does the strong relationship between moderate to exceptional summer droughts and La Niña suggest a potential role for the La Niña influence continuing into spring? How could a moderate La Niña, such as the 2010/2011 event, cause exceptional drought over Texas? We evaluated the relationship between seasonal rainfall anomalies and 2 month lead Nino3.4 indices and find that while negative rainfall anomalies in winter and spring tend to follow strong La Niñas in fall (Oct–Dec) and winter (Dec–Feb) (Fig. 9a, b), there is not a clear relationship between La Niña SSTAs during early spring (Feb–Apr) and late-spring (AMJ) rainfall anomalies (Fig. 9c). It is interesting to note that positive rainfall anomalies (sometimes exceeding 1 SD) have also occurred in all seasons during La Niña years.

The AMIP-type simulations for the La Niña SST show enhanced southeasterly winds in April (Fig. 10). The difference between the La Niña and control simulations shows an enhanced anticyclonic circulation and higher geopotential anomalies at 850 hPa over the eastern half of the US including eastern and central Texas, and southeasterly winds from the Gulf of Mexico to Texas [Fig. 10(i)(c)]. This pattern is consistent with the observed pattern of vorticity anomalies in that region (Fig. 8). The difference in geopotential height at 500 hPa between the La Niña test [Fig. 10(ii)(a)] and control run [Fig. 10(ii)(b)] shows moderately higher mid-tropospheric pressure (10 gpm), and enhanced easterly winds over Texas under La Niña conditions [Fig. 10(ii)(c)].

(i) 850 hPa geopotential height and wind vector in April



(ii) 500 hPa geopotential height and zonal wind at 850 hPa in April



(iii) Precipitation and U850 anomalies (LaTest - CTL)

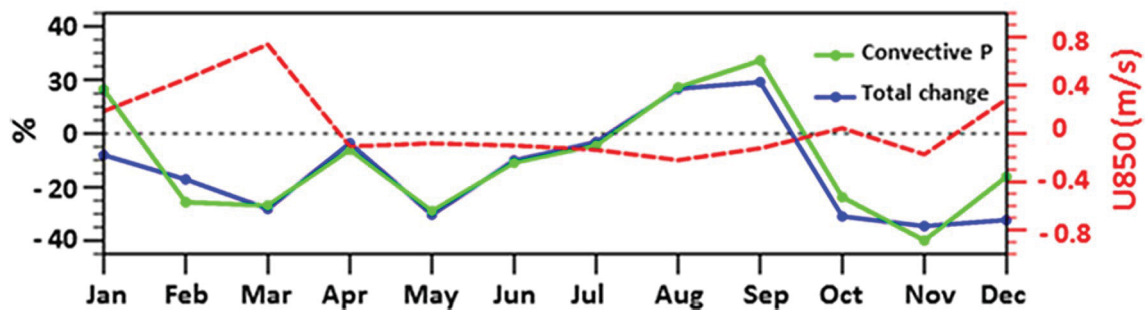


**Fig. 10** **i** Comparison of the geopotential height and mean wind vector at 850 hPa in the control [(a), CTL] and La Niña test cast [(b), LaTest] shows enhanced south easterly flow (green vectors) into Texas [(i)(c), LaTest—CTL] from the Gulf of Mexico with La Niña conditions in April. Contour interval for control and test run figures is 20 gpm, and wind unit vector is  $2 \text{ m s}^{-1}$ . Contour interval for the La Niña test minus the control run is 2 gpm and the wind unit vector is  $0.5 \text{ m s}^{-1}$ ; **ii** The enhanced easterly flow with La Niña conditions is clearly evident in the zonal component of the wind vector ( $\text{m s}^{-1}$ ; shading, positive means westerly wind and negative is easterly wind) at 850 hPa (c). The geopotential height at 500 hPa difference between the La Niña test and control run shows moderately higher pressure (10 gpm) over the entire domain with La Niña conditions [contour interval is 60 gpm in the control (a) and La Niña test (b) figures, and 10 gpm in the LaTest-CTL (c) case]; **(iii)** Domain ( $110^{\circ}\text{W}$ – $92^{\circ}\text{W}$ ,  $24^{\circ}\text{N}$ – $40^{\circ}\text{N}$ ) averaged precipitation (%) and 850 hPa zonal wind (red line,  $\text{m s}^{-1}$ ) changes for LaTest—CTL show that La Niña conditions are typically associated with enhanced westerlies (positive values of U850) from Jan–Mar (JFM) with a peak in March, weak easterly zonal winds (negative values of U850) from April through September, and a reduction in rainfall in JFM, May and Oct–Dec. The green line shows change of convective precipitation, and the blue line shows change of total precipitation

Precipitation change (%) and 850 hPa zonal wind change, averaged for the domain  $110^{\circ}\text{W}$ – $92^{\circ}\text{W}$  and  $24^{\circ}\text{N}$ – $40^{\circ}\text{N}$ , show that La Niña conditions are typically associated with enhanced westerlies (positive values of U850) from January through March with a peak in March, weak easterly zonal winds (negative values of U850) from April through September, and a reduction in rainfall in from January through March, May and October through December. Thus, the strengthened westerlies observed in April 2011, and in other moderate-to-exceptional drought years, may not be attributed to La Niña. However, increased anticyclonic circulation over the southeastern U.S. under La Niña conditions may, in part, contribute to a reduction in precipitation over eastern Texas in April.

### 3.1.3 Interaction between local surface dryness and circulation anomalies

Spring dryness usually follows the cumulative soil moisture deficits resulting from reduced precipitation from winter through spring. We investigated whether such apparent dry memory is due to the persistence of remote forcing, as represented by the autocorrelation of the pentad 500 hPa height anomalies, or land surface feedbacks, as represented by the lead-lag correlation between pentad soil moisture anomalies and 500 hPa geopotential height anomalies ( $Z'$ ) during May–July. There is a significant negative correlation between soil moisture anomalies and 500 hPa  $Z'$  2–3 week later, exceeding the autocorrelation of  $Z'$  at 500 hPa with the same phase lags (Fig. 11). This implies that dry soil moisture anomalies over the south central US could influence on positive 500 hPa height anomalies 2–3 weeks later, more so than the memory of the atmosphere either due to

internal variability or remote forcing in the late-spring/early-summer. We note that the magnitude of the correlation averaged over the 2–3-week lagged period is weak (correlation coefficient:  $-0.15$ ). This could be due to strong weather noise at pentad resolution in both fields.

In summary, the abnormally strong increase in CIN in late-spring, due to abnormally strong westerly wind anomalies and surface dryness, may have played a significant role in suppressing the late-spring rainfall over Texas in 2011, especially over western Texas where La Niña-induced circulation anomalies are weak during spring. Convective inhibition remained high until the end of June 2011 (Figs. 4, 6), and further suppressed rainfall and decreased soil moisture in the summer (e.g. Myoung and Nielsen-Gammon 2010). The persistent soil moisture deficit and higher surface temperature may have provided a positive feedback to strong mid-tropospheric ridge, which contributed to the persistence of the drought throughout the summer months.

### 3.2 Demise of the drought

Drought demise occurred in the winter of 2011/2012 (Fig. 1f), despite a second La Niña event that developed during the fall of 2011 and persisted until February 2012 (Fig. 2f). What was the forcing responsible for the demise of the drought?

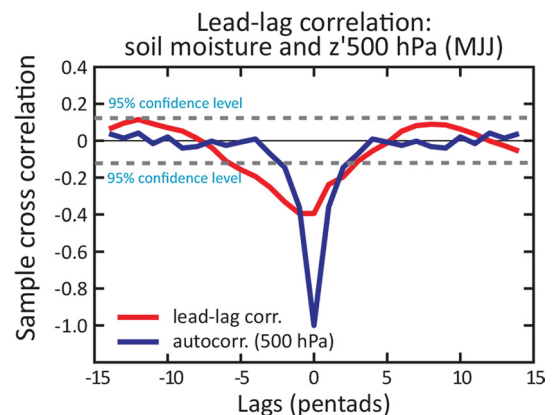


**Fig. 11** The lead-lag correlation (red line) between pentad soil moisture anomalies and 500 hPa geopotential height anomalies during May–July (MJJ) over the SC US over the period 1981–2012. The blue line depicts the autocorrelation function (ACF) of the pentad 500 hPa geopotential height anomalies of MJJ for same region and period. The ACF values have been multiplied by  $-1$  for easy comparison with the lead-lag correlation between soil moisture and 500 hPa geopotential height anomalies. The 95 % confidence bounds are derived as the standard deviations divided by the square roots of  $N$ , where  $N$  is the effective number of independent samples (Livezey and Chen 1983). The original sample size is  $n = 612$ , whereas  $N = 139$  after accounting for autocorrelation in the time series



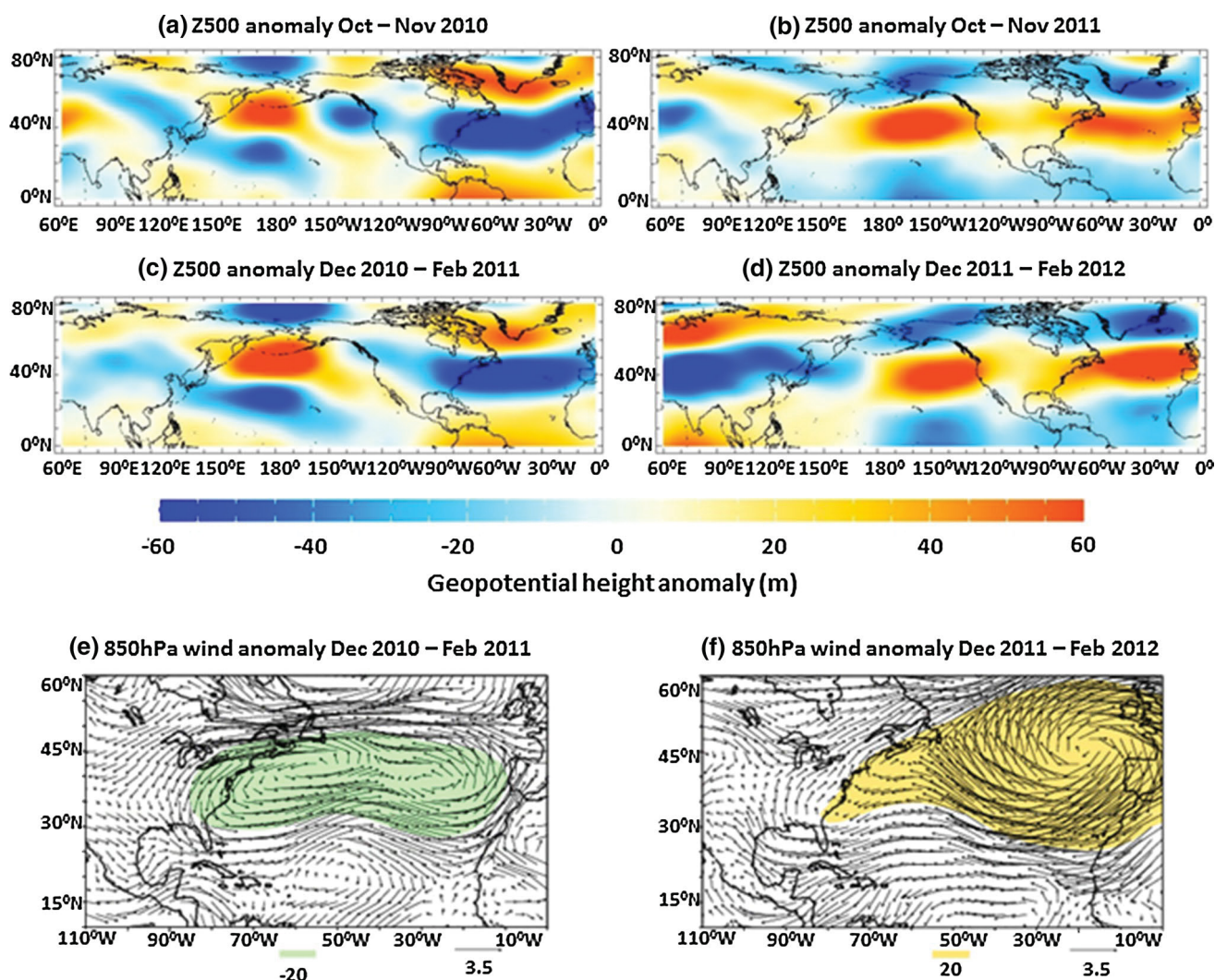


**Fig. 12** **a** 500 hPa height anomalies for Oct–Nov 2010, **b** same as **a**, but for Oct–Nov 2011, **c** 500 hPa height anomalies for DJF 2010/2011, **d** same as **c** but for DJF 2011/2012, **e** 850 hPa wind anomalies super imposed on the 850 hPa geopotential height anomalies

for DJF 2010/2011, where the 850 hPa geopotential height anomalies  $<20$  m are colored. The unit vector is  $3.5 \text{ m s}^{-1}$ , **f** same as **e** but for DJF 2011/2012, where the 850 hPa height anomalies  $>20$  m are colored

A comparison between the winter SSTAs for 2010/2011 and 2011/2012 winters shows the largest differences are in the North Atlantic. For DJF 2010/2011, there were positive SSTAs in the tropical Atlantic and over latitudes north of  $55^\circ\text{N}$  with negative SSTAs along the Atlantic coast (Fig. 2b). This pattern will have a large positive projection onto the Atlantic Multidecadal Oscillation (AMO). A positive phase of the AMO will enhance the impact of La Niña events on precipitation over the southern United States (Mo et al. 2009; Schubert et al. 2009; Pu et al. 2016). That may explain the intense dry conditions over the Southeast and eastern Texas in 2011.

The NAO was in a negative phase in the fall and winter of DJF 2010/2011 (Seager et al. 2014). This is evident from the 500 hPa geopotential height anomalies for DJF

2010/2011 (Fig. 12c), which showed positive geopotential height anomalies over Greenland, and the below-normal height anomalies over the eastern U.S. and the central North Atlantic (Fig. 12a, c). Wind anomalies at 850 hPa showed cyclonic circulation anomalies from the eastern United States to the Atlantic centered along  $40^\circ\text{N}$ , and anti-cyclonic wind anomalies to the north and south (Fig. 12e). The negative anomalies over the eastern United States were responsible for weaker low-level meridional transport from the Gulf of Mexico to the central United States. Therefore, there was less moisture transport from the Gulf to the Southern Plains and less rainfall in 2011.

For the DJF 2011/2012 season, the 850 hPa wind anomalies showed anti-cyclonic circulation in the Atlantic (Fig. 12f), consistent with the positive phase of the NAO,

with negative geopotential height anomalies over Greenland and positive geopotential height anomalies over the eastern U.S. and the central North Atlantic (Fig. 12b, d). The anti-cyclonic circulation in the Atlantic implies anomalously strong low level meridional wind. Consequently, there was stronger moisture transport from the Gulf of Mexico to the central United States, and, therefore, more rainfall over Texas and the southern Great Plains.

#### 4 Conclusions and discussion

The 2011 drought over Texas was one of strongest droughts in the state. Its most intense phase lasted from February to December 2011 and spread beyond Texas to Oklahoma, Kansas, New Mexico and Louisiana. The drought intensified rapidly in the spring of 2011, and ended in the winter of 2011/2012.

The drought intensified in the spring when SSTAs associated with the 2010/2011 La Niña event were transitioning to an ENSO-neutral state, and ended despite of the presence a La Niña, which is typically expected to result in winter rainfall deficits over Texas. We find a strong increase of CIN over the south central United State in April, which is the critical month for the onset of the main April–June rainfall season over Texas. The increase of CIN can be attributed to two factors. First, the cumulative soil moisture deficits from winter through early-spring associated with the 2010/2011 La Niña event. Second (and more directly related), the anomalously strong westerly winds in the lower troposphere in April that advected warm air from the Mexican Plateau, and contributed to an increase of temperature above the atmospheric boundary layer over Texas. We find that the strengthened lower tropospheric westerly zonal winds in April is a common phenomenon preceding past strong summer droughts with rainfall deficits extending from winter through spring over Texas.

The AMIP-type simulations using NCAR CAM5.3 suggest that La Niña conditions do not appear to explain the enhanced westerlies observed in spring, although La Niña like SSTA could enhance anticyclonic flow over the southeastern U.S., including eastern Texas. The enhanced westerly wind anomalies could be linked to the increased poleward-gradient of lower tropospheric geopotential thickness (Fig. 3b). Whether this is linked to cooler SSTAs off the west coast of U.S., which could decrease lower tropospheric thickness over northwestern U.S., needs to be investigated.

We find that soil moisture deficits appear to have a stronger correlation with the 2–3-week-lagged positive mid-tropospheric geopotential height anomalies than the autocorrelation of the latter over the south central United States in the summer. This implies that a soil moisture

deficit in the late-spring (i.e. May) may provide a positive feedback to the anomalous mid-tropospheric ridge, which contributes to drought intensification in the summer. Investigation of the underlying mechanisms of such an empirical relationship may yield new insights on the importance of soil moisture feedback to anomalous mid-tropospheric ridging, and provide the scientific basis for the early warning of strong summer droughts over the south central United States.

Drought demise occurred in the winter of 2011/2012 even though a second La Niña event developed during the fall of 2011 and persisted until February 2012. Drought demise appears to be connected to a positive NAO that drove anticyclonic circulation in the Atlantic and strengthened low-level moisture transport from the Gulf of Mexico. Above-normal winter rainfall subsequently helped relieve the drought over most of Texas. The sudden demise of the 2011 Texas drought appears to be a result of internal atmospheric variability and, thus, is intrinsically unpredictable.

**Acknowledgments** This research was supported by the Postdocs Applying Climate Expertise Postdoctoral Fellowship Program, which is partially funded by NOAA's Climate Program Office and administered by the University Corporation for Atmospheric Research (UCAR) Visiting Scientist Programs (VSP). The research was also funded by NOAA's Climate Program Office's Modeling, Analysis, Predictions, and Projections Program (Grant Award NA10OAR4310157), the Jackson School of Geosciences, and by the U.S. Army Corps of Engineers' Texas Water Allocation Assistance Program funding provided to the Texas Water Development Board. The authors thank the anonymous reviewer whose insightful comments and helpful suggestions guided a major revision of a previous version of this manuscript.

#### References

- Barlow M, Nigam S, Berbery EH (2001) ENSO, Pacific decadal variability and U.S. summertime precipitation, drought and streamflow. *J Clim* 14:2105–2127
- Benjamin SG, Carlson TN (1986) Some effects of surface heating and topography on the regional severe storm environment. Part I: three-dimensional simulations. *Mon Weather Rev* 114(2):307–329
- Dee DP, Uppala SM, Simmons AJ, Berrisford P, Poli P, Kobayashi S et al (2011) The ERA-Interim reanalysis: configuration and performance of the data assimilation system. *Q J R Meteorol Soc* 137(656):553–597
- Eichler T, Higgins W (2006) Climatology and ENSO-related variability of North American extratropical cyclone activity. *J Clim* 19(10):2076–2093
- Enfield D, Mayer DA (1997) Tropical Atlantic sea surface temperature variability and its relation to El Niño-Southern Oscillation. *J Geophys Res* 102:845–929
- Fan Y, Van den Dool H (2008) A global monthly land surface air temperature analysis for 1948–present. *J Geophys Res Atmos* (1984–2012) 113:D01103. doi:10.1029/2007JD008470
- Fannin B (2012) Updated 2011 Texas agricultural drought losses total \$7.62 billion. *AgriLifeTODAY* March 21. <http://today.agrilife.org/2012/03/21/updated-2011-texas-agricultural-drought-losses-total-7-62-billion/>

- Hoerling M, Kumar A, Dole R, Nielsen-Gammon JW, Eischeid J, Perlwitz J, Quan X-W, Zhang T, Pegion P, Chen M (2013) Anatomy of an extreme event. *J Clim* 26(9):2811–2832
- Hong S-Y, Kalnay E (2002) The 1998 Oklahoma-Texas drought: mechanistic experiments with NCEP global and regional models. *J Clim* 15:945–963
- Hu Q, Feng S (2012) AMO-and ENSO-driven summertime circulation and precipitation variations in North America. *J Clim* 25(19):6477–6495
- Kalnay E, Kanamitsu M, Kistler R, Collins W, Deaven D, Gandin L, Iredell M, Saha S, White G, Woollen J (1996) The NCEP/NCAR 40-year reanalysis project. *Bull Am Meteorol Soc* 77(3):437–471
- Koster RD, Dirmeyer PA, Guo Z, Bonan G, Chan E, Cox P et al (2004) Regions of strong coupling between soil moisture and precipitation. *Science* 305(5687):1138–1140
- Kousky VE, Ropelewski CF (1989) Extremes in the Southern Oscillation and their relationship to precipitation anomalies with emphasis on the South American Region. *Revista Brasileira de Meteorologia* 4(2):351–363
- Liebmann B, Smith CA (1996) Description of a complete (interpolated) outgoing longwave radiation dataset. *Bull Am Meteorol Soc* 77:1275–1277
- Livezey RE, Chen WY (1983) Statistical field significance and its determination by Monte Carlo techniques. *Mon Weather Rev* 111(1):46–59
- Madden RA, Williams J (1978) The correlation between temperature and precipitation in the United States and Europe. *Mon Weather Rev* 106(1):142–147
- McCabe GJ, Betancourt JL, Gray ST, Palecki MA, Hidalgo HG (2008) Associations of multi-decadal sea-surface temperature variability with US drought. *Quat Int* 188(1):31–40
- McKee TB, Doesken NJ, Kleist J (1993) The relationship of drought frequency and duration to time scales. In: Preprints, eighth conference on applied climatology. Anaheim, CA, AMS, pp 179–184
- McKee TB, Doesken NJ, Kleist J (1995) Drought monitoring with multiple time scales. In: Preprints, ninth conference on applied climatology. Dallas, TX, AMS, pp 233–236
- Mo KC, Schemm JE, Yoo SH (2009) ENSO and the Atlantic multi decadal oscillation on drought over the United States. *J Clim* 22:5962–5982
- Myoung B, Nielsen-Gammon JW (2010) The convective instability pathway to warm season drought in Texas. Part I: the role of convective inhibition and its modulation by soil moisture. *J Clim* 23:4461–4488
- Namias J (1960) Factors in the initiation, perpetuation and termination of drought. *IASH Comm Surf Waters Publ* 51:81–94
- Neale RB, Chen CC, Gettelman A, Lauritzen PH, Park S, Williamson DL et al (2012) Description of the NCAR community atmosphere model (CAM 5.0). NCAR Tech. Note NCAR/TN-486+STR
- Pu B, Fu R, Dickinson RE, Fernando DN (2016) Why do summer droughts in the Southern Great Plains occur in some La Niña years but not others? *J Geophys Res Atmos* 121. doi:10.1002/2015JD023508
- Rayner NA, Parker DE, Horton EB, Folland CK, Alexander LV, Rowell DP et al. (2003) Global analyses of sea surface temperature, sea ice, and night marine air temperature since the late nineteenth century. *J Geophys Res Atmos* (1984–2012) 108:4407(D14). doi:10.1029/2002JD002670
- Ropelewski CF, Halpert MS (1989) Precipitation patterns associated with the high index phase of the Southern Oscillation. *J Clim* 2:268–284
- Schubert SD et al (2009) A USCLIVAR project to assess and compare the responses of global climate models to drought related SST forcing patterns: overview and results. *J Clim* 22:5251–5272
- Seager R, Goddard L, Nakamura J, Henderson N, Lee DE (2014) Dynamical causes of the 2010/11 Texas-northern-Mexico drought. *J Hydrometeorol* 15(1):39–68
- Smith TM, Reynolds RW, Peterson TC, Lawrimore J (2008) Improvements to NOAA's historical merged land–ocean surface temperature analysis (1880–2006). *J Clim* 21(10):2283–2296
- Texas Water Development Board (2010) Texas Water Conditions (September 2010). [http://www.twdb.texas.gov/publications/reports/waterconditions/twc\\_pdf\\_archives/2010/twcSep2010.pdf](http://www.twdb.texas.gov/publications/reports/waterconditions/twc_pdf_archives/2010/twcSep2010.pdf)
- Texas Water Development Board (2011a) Texas Water Conditions (November 2011). [http://www.twdb.texas.gov/publications/reports/waterconditions/twc\\_pdf\\_archives/2010/twcNov2011.pdf](http://www.twdb.texas.gov/publications/reports/waterconditions/twc_pdf_archives/2010/twcNov2011.pdf)
- Texas Water Development Board (2011b) Texas Water Conditions (September 2011). [http://www.twdb.texas.gov/publications/reports/waterconditions/twc\\_pdf\\_archives/2010/twcSep2011.pdf](http://www.twdb.texas.gov/publications/reports/waterconditions/twc_pdf_archives/2010/twcSep2011.pdf)
- Ting M, Wang H (1997) Summertime U.S. precipitation variability and its relation to Pacific sea surface temperature. *J Clim* 10:1853–1873
- Trenberth KE, Shea DJ (2005) Relationships between precipitation and surface temperature. *Geophys Res Lett*. doi:10.1029/2005GL027760
- Weisman RA (1990) An observational study of warm season southern Appalachian lee troughs. Part I: boundary layer circulation. *Mon Weather Rev* 118(4):950–963
- Wilks DS (2006) *Statistical methods in the atmospheric sciences*, 2nd edn. Academic Press, New York
- Xia Y et al (2012) Continental-scale water and energy flux analysis and validation for the North American Land Data Assimilation System project phase 2 (NLDAS-2): 1. Intercomparison and application of model products. *J Geophys Res Atmos* 117(D3):D03109
- Xie PP, Chen M, Shi W (2010) CPC unified gauge based analysis of global daily precipitation. In: AMS 24th Conference on hydrology. Jan 18–21, 2010, Atlanta, GA